DØ Note 5923-CONF

Search for high-mass narrow resonances in the di-electron channel at DØ

The DØ Collaboration
URL http://www-d0.fnal.gov
(Dated: July 13, 2009)

We report a preliminary result on a search for high-mass narrow resonances decaying into two electrons, using 3.6 fb^{-1} of data collected with the DØ detector at the Fermilab Tevatron. We do not observe any excess over the standard model expectations and set a 95% confidence level upper limit on the production cross section times branching ratio for the reaction $p\bar{p} \to X \to ee$, where X is a boson with spin 1 or 2. This production cross-section limit is interpreted as lower mass limits for a variety of Z' models, and for Kaluza-Klein gravitons in the Randall-Sundrum model.

Preliminary Results for Summer 2009 Conferences

I. INTRODUCTION

High-mass neutral narrow resonances are predicted by various theories beyond the standard model (SM), in particular by theories that attempt to unify the SM forces, or attempt to explain the large difference between the SM and the gravitational energy scales.

The gauge group structure of the SM, $SU(3)_C \otimes SU(2)_L \otimes U(1)_L$, can be part of a larger gauge group like $SO(10)$, and E_6 [1] for the purpose of grand unification theories (GUT). In many models of GUT symmetry breaking, $U(1)$ groups survive at relatively low energies [2], leading to corresponding neutral heavy gauge bosons, commonly referred to as Z' bosons. Such Z' bosons typically couple to SM fermions via the electroweak interaction. They can be observed in hadron colliders as narrow resonances through the process $q\bar{q} \to Z' \to ee$.

Extra spatial dimension models provide a possible explanation for the difference between the electroweak symmetry breaking scale and the gravitational energy scale (M_{Pl}). An example of such a model is the Randall-Sundrum (RS) scenario [3] that postulates the existence of an additional spatial dimension. In the simplest form of the RS model, the only particles that propagate in the extra dimension are the gravitons G. In our three spatial dimensions, these gravitons appear as excited Kaluza–Klein modes, with each mode being a narrow spin 2 resonance. Such gravitons could be observed through the process $q\bar{q} \to G \to ee$. The parameters of the RS model are expressed in terms of the mass of the first excited mode of the graviton M_G, and the dimensionless coupling to the standard model fields, k/M_{Pl}, where k^2 is the space-time curvature in the extra dimension. This coupling constant is expected to be between 0.01 and 0.1 [4, 5].

In this note we present results on direct searches for high-mass narrow resonances via the ee final state. Currently the most stringent limits on the production of high-mass narrow resonances in the ee channel are set by the CDF collaboration using 2.5 fb^{-1} data in 2008 [6]. That analysis reports an excess over the SM prediction at an ee invariant mass of 240 GeV/c^2.

II. DØ DETECTOR AND EVENT SELECTION

The data sample used in this search was collected by the DØ detector [7], located at the Fermilab Tevatron $p\bar{p}$ Collider with a center-of-mass energy of 1.96 TeV, between July 2002 and September 2008 using a set of di-electron triggers. The total integrated luminosity for the data sample studied is measured to be (3660 ± 223) pb^{-1} [8].

The DØ detector is a multipurpose collider detector that includes a central tracking system, composed of a silicon microstrip tracker (SMT) and a central fiber tracker (CFT), both located within a 2 T superconducting solenoidal magnet and optimized for tracking and vertexing capabilities at pseudorapidities of $|\eta| < 3$ and $|\eta| < 2.5$ respectively. The pseudorapidity η is defined as $\eta = -\ln[\tan(\theta/2)]$, where θ is the polar angle with respect to the proton direction. Three liquid argon and uranium calorimeters provide coverage out to $|\eta| \approx 4.2$; the central section provides coverage of $|\eta| < 1.1$ and two end-cap calorimeters with an approximate coverage of $1.5 < |\eta| < 4.2$ for jets and $1.5 < |\eta| < 3.2$ for electrons. A muon system surrounds the calorimeter and consists of three layers of scintillators and drift tubes and 1.8 T iron toroids with coverage of $|\eta| < 2$.

This analysis is a direct extension of Ref. [9] and uses the same event selection. The event selection requires two isolated clusters of deposited energy in the central ($|\eta| < 1.1$) electromagnetic calorimeter with transverse energy above 25 GeV. The energy deposition patterns are required to be consistent with those of electromagnetic showers. Each electromagnetic (EM) cluster is required to be spatially matched to a reconstructed track. However, in the present analysis, the two candidates are not required to have opposite charge, since the probability of charge misidentification increases in the high energies studied. After applying the data selection criteria, 55711 events remain. The most energetic event has an invariant mass of 766 GeV and its display can be seen in Fig. 7.

III. BACKGROUND ESTIMATION AND NORMALIZATION

The background for this analysis can be divided into physics backgrounds, with di-electron final states, and instrumental backgrounds. The main source of physics background is the Drell-Yan (DY) production of ee pairs. The DY events are modeled using the PYTHIA [10] Monte Carlo (MC) event generator, with CTEQ6L1 [11] parton distribution functions, and then processed through the standard DØ detector simulation based on GEANT3 [12]. The MC events are processed through the same reconstruction code as the data, and pass the same selection criteria. Additionally, other SM contributions (later labelled as "other SM") from $Z/\gamma^* \to \tau^+\tau^-$, $W + X \to e\nu + X$ where X is a jet/γ misidentified as an electron, $W^+W^- \to e^+e^-\nu_e\bar{\nu}_e$, $W^{\pm}Z$ where $Z \to e^+e^-$, and $t\bar{t} \to W^+b + W^-\bar{b} \to e^+\nu_e b + e^-\bar{\nu}_e\bar{b}$ are considered.

The main source of instrumental background arises from QCD multijet events in which both jets have been misidentified as isolated electrons. It is estimated from data by selecting events which obey all the criteria except the shower shape requirement. These data are used to estimate the shape of the di-electron invariant mass spectrum of events with misidentified electrons.

The other SM background is normalized to the integrated luminosity and subtracted from the measured di-electron invariant mass spectrum. The resulting mass spectrum is adjusted to the sum of the DY and instrumental backgrounds in the region around the Z boson peak, 70 GeV/c^2 $< m(ee) <$ 150 GeV/c^2. The fit uses the shapes of the DY, and the instrumental backgrounds to determine their relative fraction in this mass region where we expect negligible contribution from new physics. The invariant mass spectra for data and for the fitted background is shown for masses in the fit region, in Fig. 1. There is good agreement between the shapes of the measured data and the sum of the backgrounds in the low mass region used for normalization.

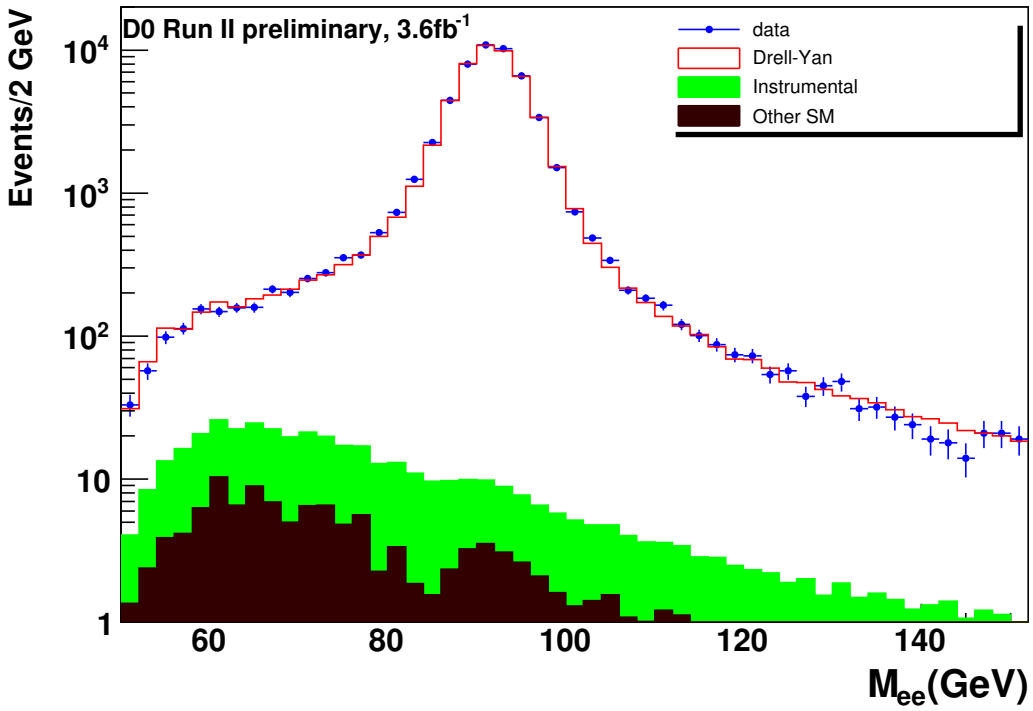

FIG. 1: Invariant mass spectrum of ee pairs for data (blue points), with expected total background and the contributions from instrumental and other SM background superimposed in the normalization region.

IV. ANALYSIS OF HIGH MASS REGION

Having normalized the backgrounds to data in the mass region around the Z boson peak, the expected background contributions are extrapolated to higher masses using the modeled di-electron mass distributions. The total background is then compared to data to search for evidence of a heavy narrow resonance. In Fig. 2, the ee invariant mass spectrum is shown for the full region analyzed with contributions of each background source.

The search for high mass resonances decaying to di-electrons, conducted by CDF, using 2.5 fb^{-1} of data, shows its largest discrepancy with the expected background at $m_{ee} \sim 240$ GeV [6]. Figure 3 shows our results for the region of the excess reported by CDF. Good agreement in that range between the data and the expected total background is observed. Furthermore, Fig. 2 shows reasonable agreement between data and expected total background for the full mass range studied. Since no significant excess is observed, an upper limit on the production cross-section is set.

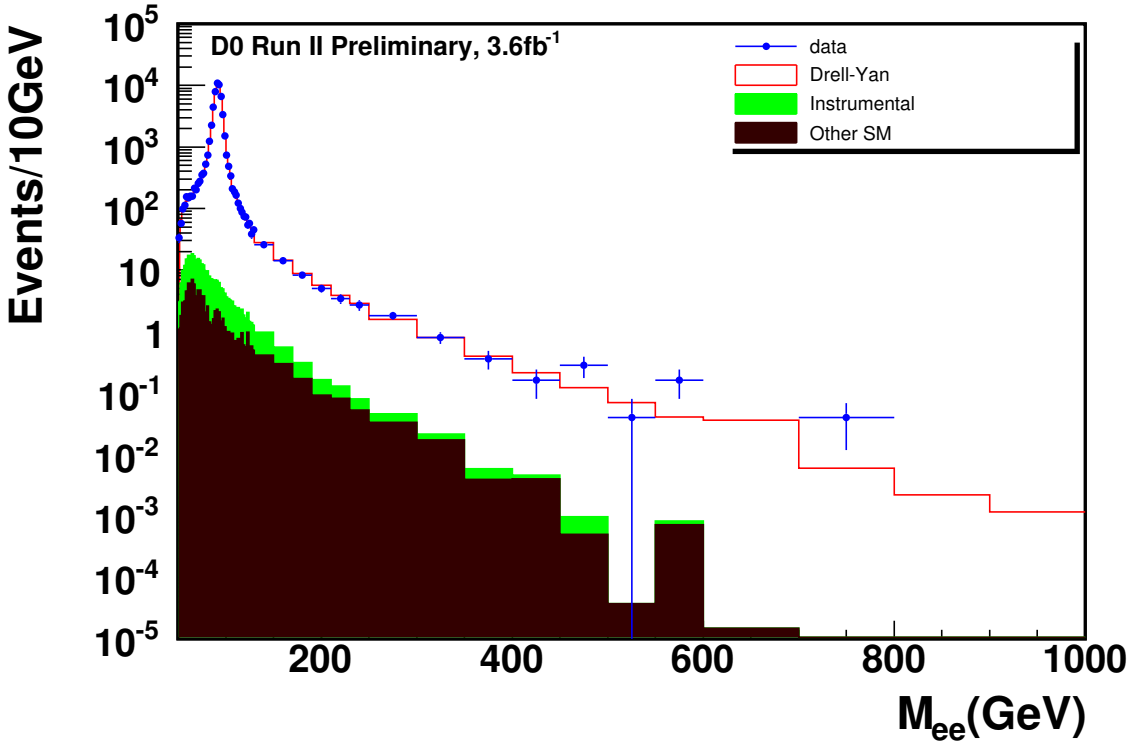

FIG. 2: Invariant mass spectrum of ee pairs for data (blue points), with expected total background and the contributions from instrumental and other SM background superimposed for the full range studied.

V. LIMIT CALCULATION

In the absence of a heavy narrow resonance signal, an upper limit on $\sigma \cdot BR(p\bar{p} \rightarrow X \rightarrow ee)$, where X is a boson with spin 1 or 2, is set. A Bayesian approach with a flat prior is used to set the limit, according to the procedure described in Ref. [13]. The inputs to the limit calculator, for a given Z' mass, are N_W, the number of observed data events in a mass window and its Poisson uncertainty, b, the number of expected background events in the same mass window, ϵ, the total signal acceptance, $\mathcal{L}$, the integrated luminosity, and the uncertainties on b, ϵ, and $\mathcal{L}$.

In order to study ϵ, the sequential standard model (SSM) Z' [14] resonance was chosen. The SSM Z', namely a Z' boson with SM couplings, is often used for convenience in comparing experimental data with theoretical prediction [15]. The width of a SSM Z' boson is proportional to the width of the Z boson, scaled by the ratio of their masses $\left(\Gamma(Z') = \Gamma(Z) * \frac{m(Z')}{m(Z)}\right)$. SSM $Z' \rightarrow ee$ samples were generated for various mass points using PYTHIA[10], processed through the standard DØ detector simulation, and passed through the same reconstruction chain as data events.

For each of the MC generated SSM Z' samples, the reconstructed ee invariant mass spectrum is fitted with a Gaussian to determine the signal reconstruction efficiency as well as the reconstructed mass and resolution. The mass resolution is 15.3, 24.9, 31.2 GeV/c^2 for invariant masses of 400, 750, 1000 GeV/c^2 respectively. Fits with a Breit-Wigner shape convoluted with a Gaussian are also performed, but do not significantly alter the results.

The systematic uncertainties considered for the signal reconstruction efficiency include the error due to PDFs that ranges from 0.3% to 7.7% (400 – 1000 GeV/c^2), the error due to the mass window selection that ranges from 0.9% to 5%, the error from the fit performed that ranges from 0.6% to 7%, and the 3% uncertainty in the electron identification efficiency. The systematic uncertainties considered for this analysis are summarized in Table I.

To quantify the results of the search for high mass narrow resonances production, the numbers of observed and expected background events are counted within a mass window defined around each input mass. For this analysis an asymmetric mass window between 3σ below the resonance mass and infinity is used, where σ is the width of the Gaussian fit of the reconstructed ee invariant mass spectrum.

The inputs to the limit calculator are summarized in Table II. The results of the 95% confidence-level limit calculation are listed in the Table III.

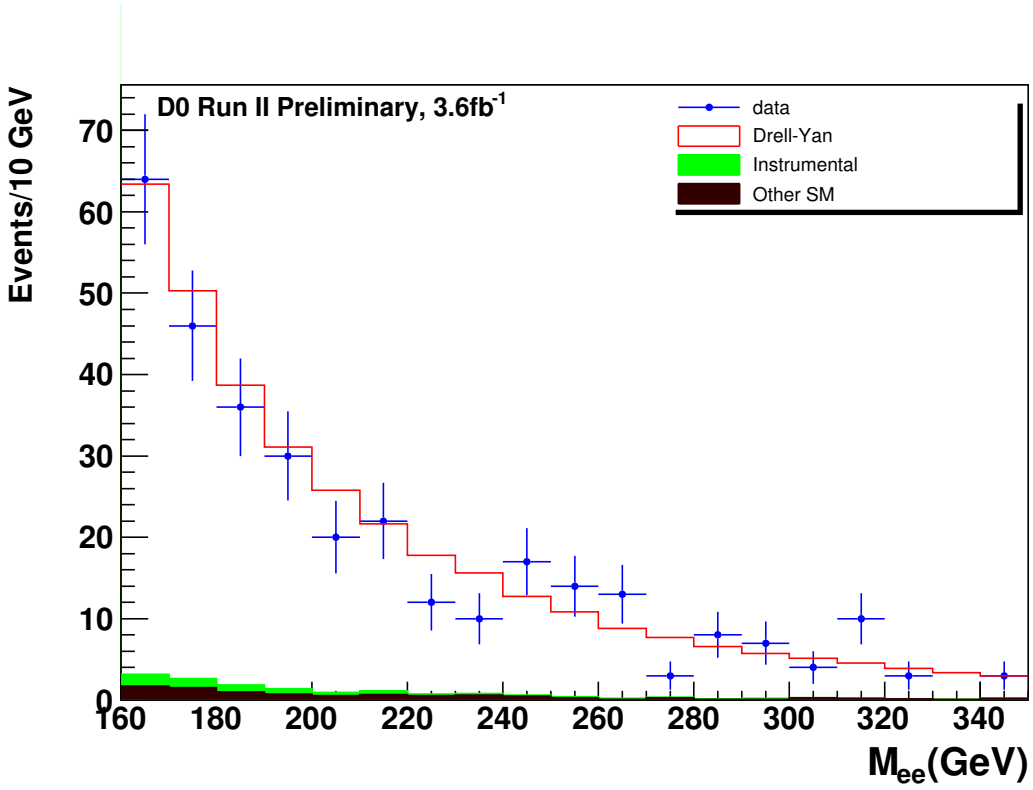

FIG. 3: Invariant mass spectrum of ee pairs for data (blue points),with expected total background and the contributions from instrumental and other SM background superimposed in the region between 160 and 350 GeV/c^2 for the full data sample analyzed.

TABLE I: Sources of uncertainty for signal acceptance and expected background.

Uncertainties for expected background	
Electron identification	3.0%
Normalization factor	0.26%
Luminosity [a]	6.1%
Cross section [b]	1.4% – 14.75%
Uncertainties for signal acceptance	
PDF	0.3% – 7.7%
Fit Error	0.6% – 7%
Window Selection	0.9% – 5%
Electron identification	3.0%

[a]Luminosity and cross section uncertainties are applied only to the SM background.
[b]Cross section uncertainties for different SM background processes: $Z \to \tau\tau$: 3.54%, $W + X$: 5.1%, WW: 6.6%, WZ: 1.4%, $t\bar{t}$: 14.75%.

Figure 4 shows the expected and observed 95% confidence-level upper limits on $\sigma(p\bar{p} \to X) \times BR(X \to ee)$ as a function of the X mass.

The 95% confidence level upper limit on production $\sigma \times BR(X \to ee)$ can be interpreted in a lower mass limit for a variety of models. For this the theoretical signal production cross-section is needed. The theoretical signal production cross section is superimposed on the calculated upper cross section limit at 95% CL, and the intersection of the graphs gives the minimum allowed mass that a Z' from a specific model can have. The theoretical signal production cross section is estimated by multiplying the leading order (LO) calculation from PYTHIA [10] by a mass independent k–factor of 1.3 [16]. To compensate for a slight mass dependence a systematic uncertainty of 8% is introduced. The theoretical cross section is shown as a band, wherever possible. In the case where many models are superimposed, only the central value of the theoretical cross section band is drawn. The intersection of the central value with the calculated upper cross section limit at 95% CL is used to determine the nominal limit. For a conservative limit the

TABLE II: Numbers of expected and observed events in different mass windows, and signal acceptance.

$M_{Z'}$ (GeV/c^2)	Mass Window Lower limit (GeV/c^2)	Data Events	Expected Background Events	Signal Acceptance
400	354	27	22.4 ± 0.7	0.172 ± 0.014
500	445	16	7.92 ± 0.22	0.188 ± 0.015
600	536	7	2.93 ± 0.07	0.199 ± 0.016
700	626	2	1.052 ± 0.025	0.207 ± 0.017
750	673	2	0.631 ± 0.016	0.209 ± 0.017
800	718	1	0.384 ± 0.010	0.211 ± 0.018
850	762	1	0.222 ± 0.006	0.212 ± 0.018
900	810	0	0.134 ± 0.004	0.216 ± 0.019
950	858	0	0.0701 ± 0.0023	0.214 ± 0.019
1000	902	0	0.0410 ± 0.0015	0.216 ± 0.021

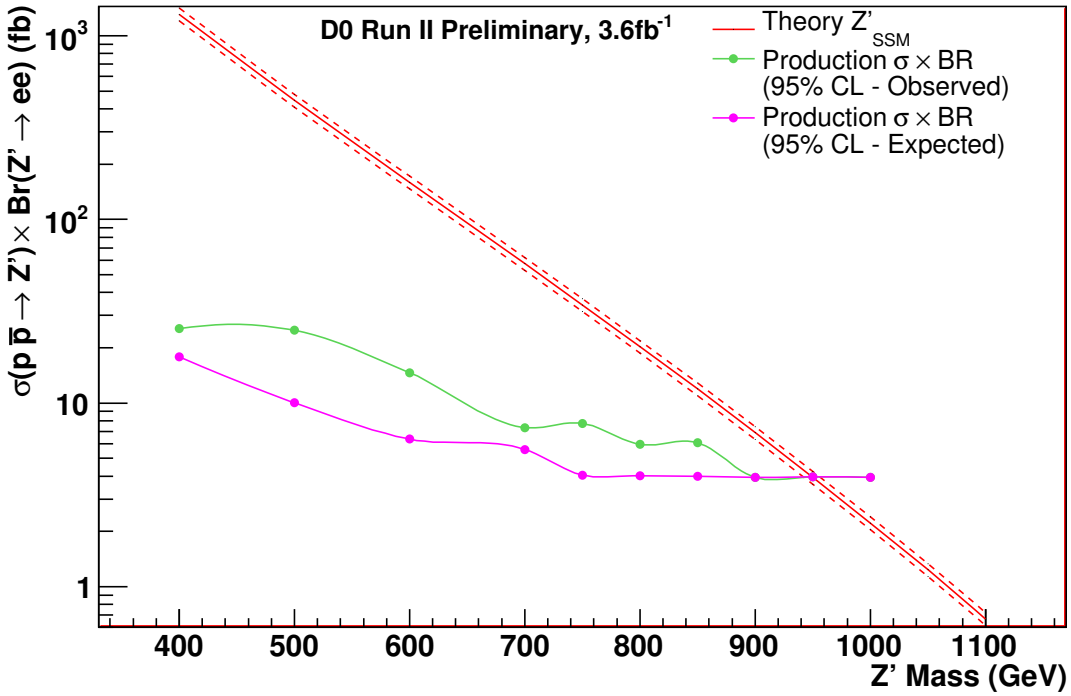

FIG. 4: 95% CL limit on $\sigma \times BR(X \to e^+e^-)$, where X is a high-mass neutral narrow resonance. The theoretical cross-section of the SSM Z' with its uncertainty is included for comparison

TABLE III: Expected and observed 95% confidence level upper limits on production $\sigma \times BR$.

Mass (GeV/c^2)	Expected Limit on Production $(\sigma \times BR)$(fb)	Observed Limit on Production $(\sigma \times BR)$(fb)
400	17.89	25.36
500	10.02	24.89
600	6.36	14.65
700	5.59	7.35
750	4.05	7.74
800	4.02	5.95
850	3.99	6.07
900	3.94	3.94
950	3.96	3.96
1000	3.94	3.94

lower edge of the theoretical cross section band is used.

As an example of spin-1 neutral narrow resonances, lower mass limits are set for the SSM Z' and the E6 Z' models (Fig. 5). The couplings for the E6 Z' models are based on Ref. [17]. Additionally, assuming the same acceptance for spin-2 neutral narrow resonances, RS gravitons with $k/M_{Pl} = 0.1$ and 0.7 are selected (Fig. 6). The results are summarized in Table IV, where each model is shown with corresponding "Expected" and "Observed" lower mass limits.

TABLE IV: Expected and observed lower mass limits for the SSM Z', E6 Z' models, and RS gravitons.

Model	Nominal		Conservative	
	Expected Lower Mass Limit (GeV/c^2)	Observed Lower Mass Limit (GeV/c^2)	Expected Lower Mass Limit (GeV/c^2)	Observed Lower Mass Limit (GeV/c^2)
Z'_{SSM}	949	950	942	944
Z'_{η}	844	810	837	800
Z'_{χ}	834	800	827	787
Z'_{ψ}	817	763	809	751
Z'_{sq}	774	719	767	713
Z'_{N}	803	744	796	736
Z'_{I}	732	692	716	683
RS ($k/M_{Pl} = 0.1$)	826	786	819	767
RS ($k/M_{Pl} = 0.07$)	767	708	758	700

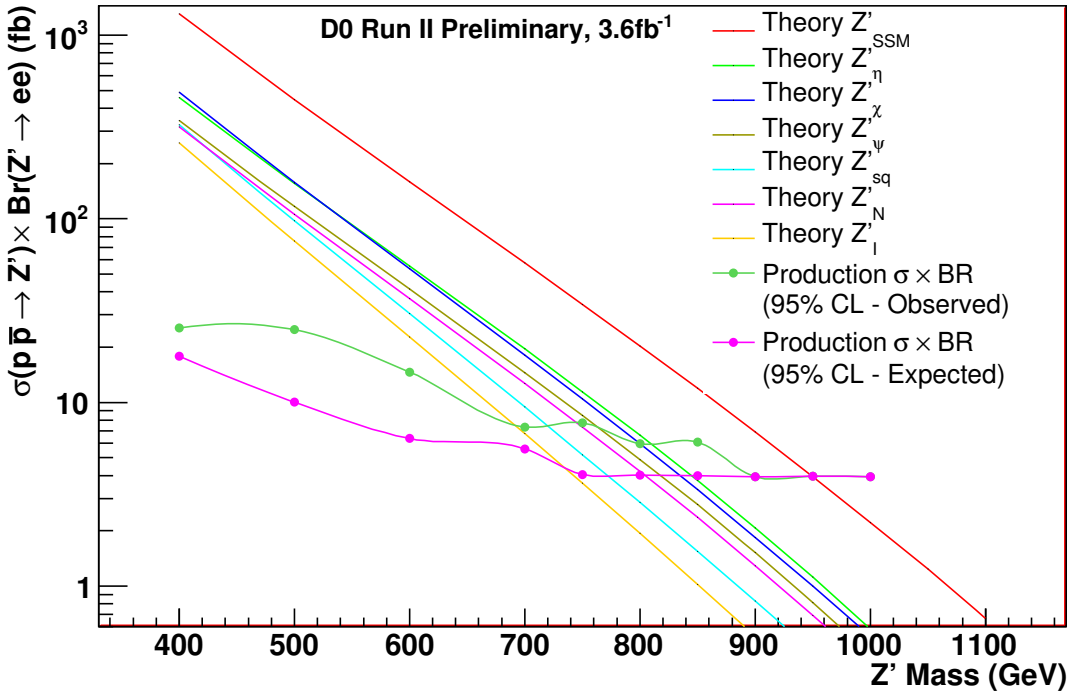

FIG. 5: The upper limit on the observed and expected cross section at 95% CL with superimposed the SSM Z', and E6 Z' models.

VI. CONCLUSION

Using 3.6 fb^{-1} of data collected with the DØ detector at the Fermilab Tevatron, we have performed a search for high mass narrow resonances X decaying via $X \to e^+e^-$. We found the di-electron invariant mass spectrum in good

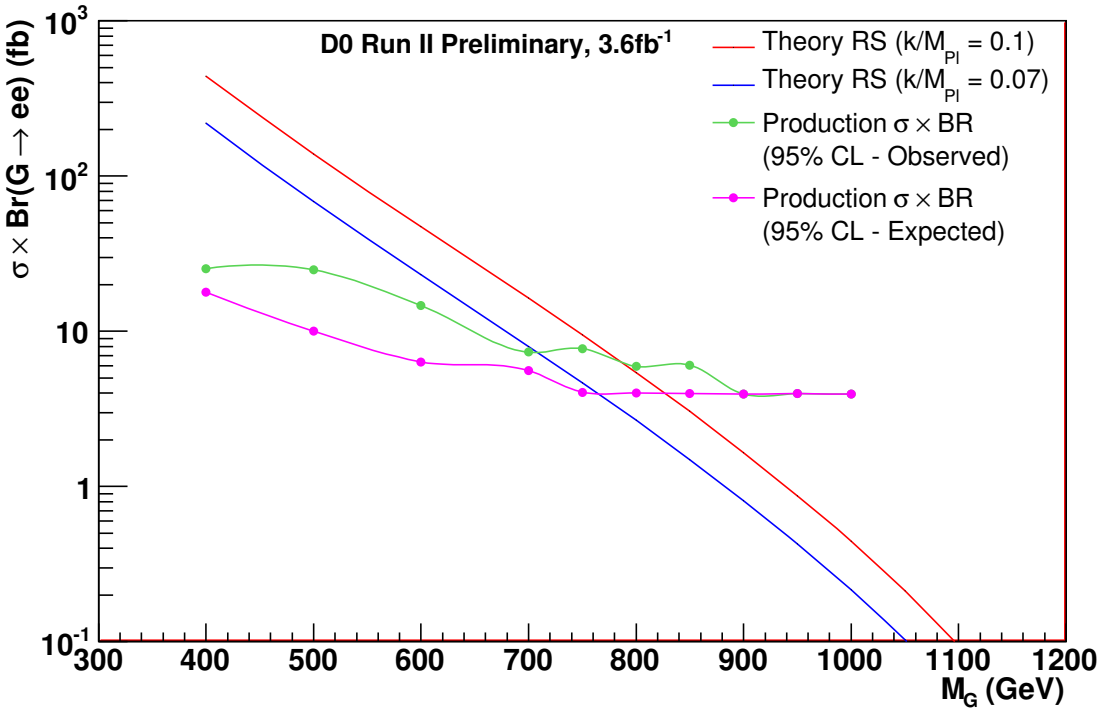

FIG. 6: The upper limit on the observed and expected cross section at 95% CL with superimposed Randall-Sundrum graviton models.

agreement with the total background expected from SM processes and instrumental backgrounds. No evidence is observed for physics beyond the SM. This preliminary result is based on the event selection from Ref. [9], designed to minimize the systematic uncertainty on the forward–backward charge asymmetry measurement. An event selection designed for maximal acceptance is being developed and expected to significantly improve the sensitivity of this analysis.

Acknowledgments

We thank the staffs at Fermilab and collaborating institutions, and acknowledge support from the DOE and NSF (USA); CEA and CNRS/IN2P3 (France); FASI, Rosatom and RFBR (Russia); CNPq, FAPERJ, FAPESP and FUNDUNESP (Brazil); DAE and DST (India); Colciencias (Colombia); CONACyT (Mexico); KRF and KOSEF (Korea); CONICET and UBACyT (Argentina); FOM (The Netherlands); STFC and the Royal Society (United Kingdom); MSMT and GACR (Czech Republic); CRC Program, CFI, NSERC and WestGrid Project (Canada); BMBF and DFG (Germany); SFI (Ireland); The Swedish Research Council (Sweden); CAS and CNSF (China); and the Alexander von Humboldt Foundation (Germany).

[1] J.L. Rosner, Phys. Rev. D**35**, 2244 (1987).
[2] P. Langacker, arXiv:0801.1345 [hep-ph] (2008).
[3] L. Randall, R. Sundrum, Phys. Rev. Lett. **83**, 3370 (1999).
[4] H. Davoudiasl, J.L. Hewett, T.G. Rizzo, Phys. Rev. Lett. **84**, 2080 (2000).
[5] H. Davoudiasl, J.L. Hewett, T.G. Rizzo, Phys. Rev. D**63** (2001) 075004.
[6] T. Aaltonen *et al.* (CDF Collaboration), Phys. Rev. Lett. **102**, 031801 (2009).
[7] V. Abazov *et al.* (DØ Collaboration), Nucl. Instum. Methods A **565**, 463 (2006).
[8] T. Andeen *et al.*, FERMILAB-TM-2365 (2007).
[9] V. Abazov *et al.* (DØ Collaboration), Phys. Rev. Lett. **101**, 191801 (2008).

[10] T. Sjöstrand *et al.*, Comput. Phys. Commun. **135**, 238 (2001).
[11] J. Pumplin *et al.*, JHEP **07**, 012 (2002).
[12] R. Brun and F. Carminati, CERN Program Library Long Writeup W5013, 1993 (unpublished).
[13] I. Bertram *et al.*, FERMILAB-TM-2104 (2000).
[14] S. Dimopoulos and H. Georgi, Nucl. Phys. **B193**, 150 (1981).
[15] M. Svetic and S. Godfrey, arXiv:hep-ph/9504216, (1995).
[16] M. Carena, A. Daleo, B. Dobrescu, and T. Tait, Phys. Rev. D **70**, 093009 (2004).
[17] C. Ciobanu *et al.*, http://www.hep.uiuc.edu/home/catutza/nota12.ps (2005).

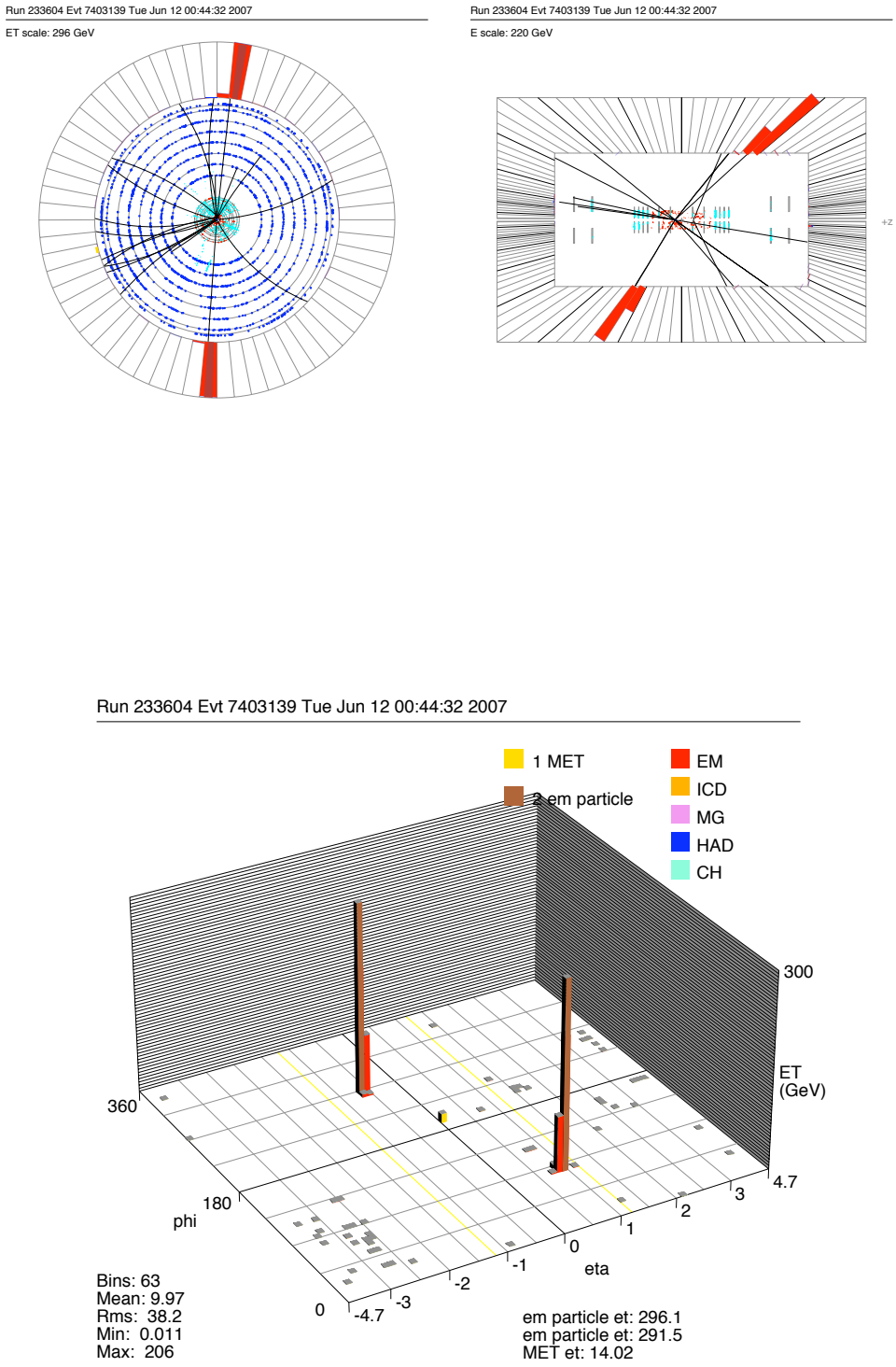

FIG. 7: Event display for the di-electron event with the highest invariant mass recorded ($M_{ee} = 766$ GeV/c^2).